

X-ray diagnostics applied to high pressure cryogenic sprays

B.Métay*, E.Robert, R.Viladrosa, M.Dudemaine, C.Cachoncinlle, J.M.Pouvesle
GREMI, CNRS/Université d'Orléans, BP 6744, 45067 Orléans cedex 2, France

W.O.H.Mayer, G.Schneider
DLR, German Aerospace Center, Lampoldshausen, 74239 Hardthausen, Germany

I.Gökalp
LCSR, EPEE, CNRS 45071 Orléans CEDEX 2- France

Abstract

The use of optical methods for the investigations of dense sprays or high density jets is limited. Light sheet methods (LIF, Raman , etc ..) are only of qualitative nature when the gradients of refractive index is high as in e.g in the core region of diesel jets or in propellant flows. A new table top flash x-ray device has been designed, developed, and used successfully for the investigation of such high density flows. Real time soft x-ray radiography allow the collection of quantitative data which are described in this paper. The paper also describes the full experimental set-up, measurement method (analysis, uncertainty and first results), and comparison with other methods.

1. Introduction

The applicability and limitations of optical methods for dense spray characterisation have been demonstrated by various authors [1-2]. While the main part of the flow is fully characterised using optical diagnostics, these techniques fail in the near nozzle region due to physical processes such as light focusing, scattering, absorption, etc. Therefore in various combustion or propulsion studies, x-ray based diagnostic methods have been developed in the last years [3-9].

Flash x-ray radiography studies have been performed for the diagnostics of liquid jet injection in a high pressure reactor [3,4]. In these studies, the liquid jet is seeded with an additive (of high atomic number) to enhance the x-ray absorption and consequently the radiographic contrast. Unfortunately, the use of an additive in the jet may involve some modification of the injection mechanism. The use of flash and soft x-ray radiography appears of peculiar interest for the really non intrusive diagnostic of dense flow composed of light atomic number elements [5]. Impressive time resolved x-ray radiography results have been recently published showing evidence of shock waves generated by high pressure fuel sprays using the Advanced Photon Source and the Cornell High Energy Synchrotron Source [6].

This paper deals with the application of flash soft x-ray radiography for the diagnostic of high pressure cryogenic sprays. In this work, a table-top flash x-ray system has been optimised for its operation at the cryogenic injection test facility of the Deutsche zentrum für

* Email : Brice.Metay@univ-orleans.fr

Luft und Raumfahrt (DLR) in Lampoldhausen. Beyond the recording of near nozzle radiographs over an extended range of spray temperature and pressure, quantitative data have been obtained and compared with the results of previously performed optical measurements and computational fluid dynamic simulations. After a description of the experimental set-up, typical radiographs are presented. The density calculation algorithm, the x-ray spectrum determination and the density results are then presented and discussed.

2. Experimental set-up

2.1 Overview

The experiment articulates around three assemblies presented in figure 1 and described in the following section : the compact flash x-ray source, the cryogenic injection installation and an X-ray detector. Each assembly has been tested separately and matched for nitrogen jet radiographic diagnostic.

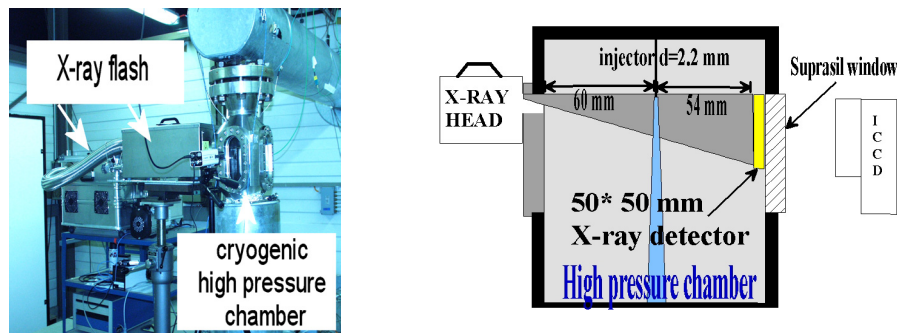


Figure 1, on left : overview of experimental set-up, on right : schematic drawing of x-ray acquisition

2.2 experimental set-up

The Lampoldhausen M51 facility allows to study the expansion of a non reactive cryogenic jet in a high pressure chamber. For this feasibility tests, a single injector of diameter $d=2.2\text{ mm}$ was used to inject a cryogenic nitrogen jet (temperature range : 100-130 K) in a 12 cm diameter high pressure nitrogen chamber that could be filled up to 6.0 MPa .To obtain a significant x-ray transmission of the entrance window, one of the 4 Suprasil® windows of the high pressure chamber was replaced by a Mylar® foil (320 μm thick, 9 mm in diameter) inserted in a thick aluminum piece. The diameter of this Mylar® window was chosen as large as possible to achieve a large field of view at the nozzle exit (22 mm, ie. $x / d = 10$ with x being the longitudinal coordinate) while allowing to withstand the nitrogen pressure up to 6.0 Mpa.

The radiographs have been obtained with two detectors: 3200 ISO black and white films and a Amorphous Carbon Scintillator (ACS) imaged with an ICCD camera mounted with a 60 mm lens. In both cases, the detector was set close to the Suprasil® output window to avoid as possible the disturbance of the flow conditions. The ACS detector has been preferred for its high sensitivity and to reduce time lag between each x-ray acquisitions. The x-ray radiography experiments at M 51 have been performed using a new pulsed, table top

(about 0.33 m^3 , 50 kg) and soft x-ray flash inspired from previous development[10]. The use of short x-ray pulse (20 ns FWHM) allow to reduce the blur due to the jet motion (few μm) during exposure to a negligible value.

The core of the x-ray diagnostics of liquid jets expanding in a high pressure chamber relies in the registration of the x-ray transmission contrast between the jet and the surrounding. The transmission factor of the x-ray photons through an object depends both on the nature and density of the object and on the energy of the x-ray photons. The figure 2 presents 4 x-ray transmission curves corresponding to the propagation through : 2.2 mm thick liquid nitrogen layer, 6 cm thick high pressure nitrogen layer, 7 cm thick Suprasil® window and 320 μm thick Mylar® window.

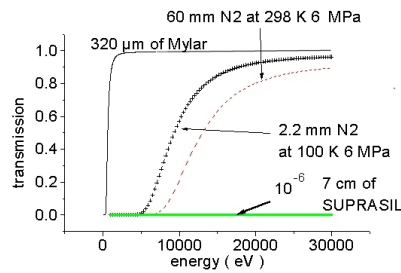


Figure 2 : transmission evolution versus photon energy through : cryogenic jet, high pressure chamber, Suprasil® window, and Mylar® window. Data from NIST [11]

The x-ray range between 7 to 20 keV appears as the x-ray energy window suitable for nitrogen jet diagnostic at high nitrogen pressure. Photons with energy lower than 7 keV are strongly absorbed by gaseous nitrogen layer before they can interact with the liquid jet. On the other hand, the liquid jet is almost transparent to photons with an energy higher than 20 keV. Therefore, the x-ray flash is operated at low voltage across the x-ray diode (< 50 kV) and with a tungsten anode. This results in the emission of the L line of W (L_{α} at 8.33, 8.39 keV L_{β} at 9.67, 9.9 keV) and a Bremsstrahlung continuum extending up to about 50 keV. The high dose rate of 1 R/shot at the x-ray head output window and x-ray focus of the few hundreds μm in diameter are also optimized for this application. Finally, the x-ray flash was operated from a remote control board and synchronized with ICCD camera. The radiograph experiments were performed with an average over 200 shots for one pressure and temperature injection condition. The preliminary test were performed in GREMI to check the operation of the x-ray source over few thousands shots. The repetition rate of the radiography experiments was limited to 5 Hz due to the camera data transfer speed. The flash X-ray source used for the radiography was placed perpendicularly to the jet axis, the x-ray focus being aligned with the nozzle tip. The distance between the x-ray focus and the jet was fixed by the chamber size and the equals to 90 mm.

3. Qualitative observations

The first experiment at M51 have been performed to check the feasibility of jet radiography in the typical cryogenic jet injection conditions (1.0 –6.0 Mpa , 100-130K). Both detection techniques (film and ACS) have been proven to be efficient and the x-ray images, presented in figure 3, of the cryogenic jet have been obtained for the first time to our knowledge. The

use of ACS / ICCD detector allowed to obtain image with very low x-ray dose (few tens of mrad at the position of scintillator located 5.4 cm away from the injector nozzle) for all conditions. Both 200 shot average radiographs, for comparison of the obtain measurement x-ray data with other average techniques (in particularly Raman diagnostic), and single shot radiographs have been performed. Single shot and 200 shot radiographs reveals no significant difference in the shape of the jet that appears has a cylinder over the first 22 mm at the nozzle exit.

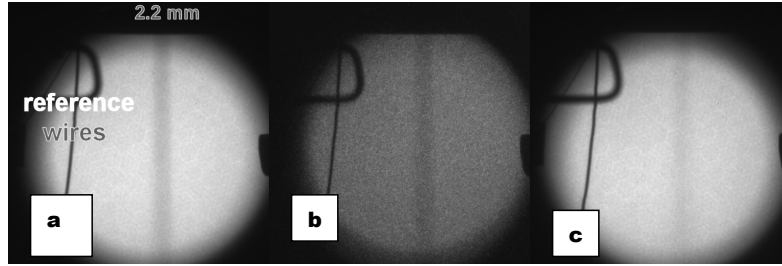


Figure 3 : X-ray ACS images of : -a- 200 shots accumulation image of jet at 100 K, 1.0Mpa
-b- single shot image of jet at 100 K, 1.0 Mpa,
-c- 200 shots accumulation image of a jet at 120 K, 6.0 Mpa

4 . density measurement

4.1 density calculation algorithm

The radiography experiments performed with the ACS detector in combination with the ICCD camera result in the recording of images 512*512 pixels in size and coded in 8 bit grey levels. The grey level value on each detector pixel depends on the x-ray propagation path from the x-ray source focus to the pixel. During their propagation, part of the x-ray photons is absorbed through the high pressure chamber and the liquid nitrogen jet. The figure 4 illustrates the x-ray propagation from the source focus to the detector. The jet, whose geometry is assumed to be cylindrical (as observed in figure 3), is analysed as a set of isodensity concentric rings. The thickness of these rings is determined by the pixel size and geometrical considerations, their density being calculated from the outermost ring to the core of the jet.

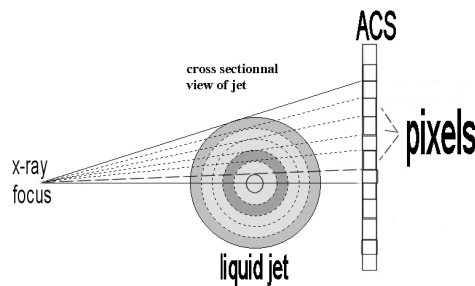


Figure 4 : schematic of ring analysis of the jet for density calculation

The transmission of the x-ray photons through the matter follow the **Beer-Lambert Law** as described in eq. 1 :

$$T = \frac{\int_{E_{\min}}^{E_{\max}} I(E) * e^{-\sigma(E) * \rho * l} dE}{\int_{E_{\min}}^{E_{\max}} I(E) dE} \quad (1)$$

where ρ is the density of the medium, l its thickness, σ its mass attenuation coefficient ($[g \cdot cm^{-2}]$), E the x-ray photons energy and $I(E)$ x-ray photon distribution function.

σ values are tabulated on the NIST web site [11]. For a monochromatic irradiation, the density is analytically inferred from the transmission value as shown in eq. 2 :

$$\rho = \frac{\ln\left(\frac{1}{T}\right)}{\sigma * l} \quad (2)$$

A lab-developed software was previously used and applied for axisymetrical jet and monochromatic spectrum [5].

For liquid nitrogen radiograph analysis both the high pressure chamber and the liquid jet absorption are strongly dependent on the X-ray photon energy (see figure 2). In this case of polychromatic spectrum, the density can not be easily deduced from the measurement of the transmission. A new routine was added to the density calculation algorithm[12]. The experimental measurement of the flash x-ray spectrum, described in the next section, allow the determination of the density by numerical calculation. The transmission is calculated taking into account the x-ray spectrum, the geometrical configuration and over the density range extending from 0 to 1000 $kg \cdot m^{-3}$ with a step of 20 $kg \cdot m^{-3}$. The density value in best agreement with the measured transmission is thus deduced from the calculation.

4.2 Experimental x-ray spectrum measurement

The flash x-ray spectrum shape has a strong influence on the density calculation. Therefore an experimental measurement of this spectrum has been performed using Ross filter characterisation method. The transmission through nine Ross filters, composed of Ag, Al, Co, Mo, Fe, Zn, Cu, W, Co, Pb, Gd thin foils have been measured and compared to their theoretical value in the x-ray energy range for which they are designed. The figure 5 presents the experimental data obtained using this method together with the fit deduced from this experiment. As expected, the spectrum is composed of the L characteristic lines of tungsten superimposed over a Bremsstrahlung continuum. The Bremsstrahlung continuum part of the spectrum has been fitted using Kramers formalism and the theoretical transmission curves of the X-ray diode output window as depicted in [13]. In our experiment the x-ray output window consists in a Mylar and an aluminium foils. One of the Ross filter allows to estimate the x-ray flux radiated in the $L\alpha$ lines at 8.4 keV. The relative intensities of the other L lines of tungsten is deduced from the calculation reported in [13]. It must be pointed out that in figure 5, the spectral intensity is expressed as the number of x-ray photons integrated over a

0.1 keV energy domain. The same energy step is considered in the density calculation algorithm.

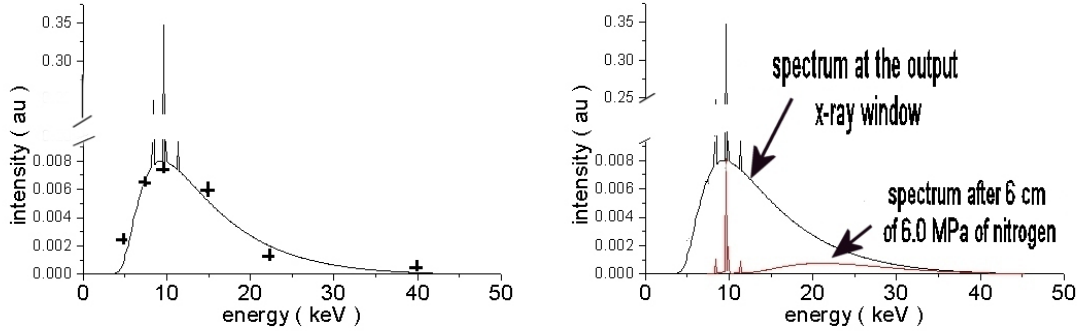


Figure 5 : left: comparison between Ross filter data (cross) and spectrum calculation , right : calculation of spectrum evolution in a high ambient gas pressure

The figure 5 illustrates the strong influence of high pressure of nitrogen in the chamber on the x-ray spectrum. While the spectrum entering the high pressure chamber is peaked around 10 keV, the x-ray spectrum at the position of the liquid nitrogen jet is peaked around 21 keV. This shift of the spectrum peak position results from the x-ray energy dependent absorption of the 6 cm thick high pressure nitrogen layer located between the entrance window and the jet nozzle. The spectrum shape is also modified across the liquid jet and the nitrogen layer in front of x-ray detector.

The theoretical transmission of Mylar® scales irradiated by photons distributed according to the x-ray flash spectrum presented in the figure 5, has been calculated and compared with experimental data as presented in figure 6.

The experimental data in figure 6a, correspond to the measurement of the transmission of three level Mylar® scale of 1.28 mm of thickness, while those in figure 6b represent the transmission of the same Mylar® scale located behind a 5.76 mm thick Mylar® foil. The 5.76 mm foil has very similar transmission curve than a 11 cm thick, 6.0 MPa nitrogen layer. The good agreement achieved through this test experiment indicates that the x-ray spectrum determination is correct.

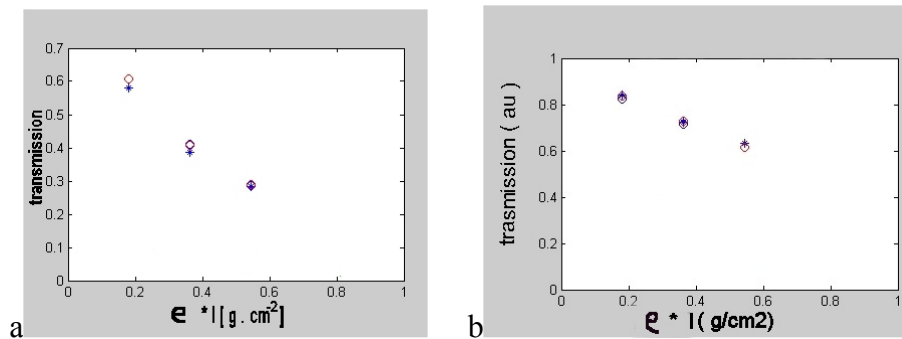


Figure 6 : comparison of data (circles) and calculation (stars) transmission of Mylar® scale irradiated by : -a- x-ray flash photons, -b- x-ray flash photons filtered through a 5.76 mm thick Mylar® foil

4.3 result

A slight modification of the x-ray spectrum was performed to achieve a 90% agreement between the density deduced from measurement at the nozzle tip with the theoretical value for one temperature and one pressure of injection. This modification of the x-ray spectrum account for the thin tungsten deposition layer observed after a few hundreds of shot of the x-ray diode on the Mylar® output window. It has been measured that after this adjustment, the density of the nitrogen jet at the nozzle tip deduced from the radiographs is in agreement with the theoretical value with in 10% for all other temperature and injection pressure. This indicates that no reference point is required for the density determination as soon as the transmission of a calibrated object has been measured. It must be pointed out that this 10% of deviation for the density value results from a transmission value deviation of only about 1%.

The evolution of the density along the jet propagation path is plotted in figure 7a and 7b following two different methods. In figure 7a, the jet is considered has a homogeneous cylinder 2.2 mm in diameter and the density value deduced from transmission value corresponds to the average density in the radial direction. In figure 7b, the jet is analysed as a set of concentric rings and the density value on the axis is calculated considering the density gradients across the radial direction. In figure 7c, both Raman measurement and simulation results are plotted for the same injection condition than in figure 7a and 7b (6.0 MPa, 120 K)[14].

There exists some agreement between the rather flat profile of the density in figure 7a and the simulation predictions. No significant density decrease was deduced from the x-ray experiment up to $x/d=10$ as was indicated by Raman measurement. The stronger oscillation of density value in figure 7b than in figure 7a probably result from the algorithm limits when considering the jet as a serie of different rings. In this first experimental campaign, the size of the x-ray scintillator and the geometrical characteristics lead to a rather limited sampling of the jet transmission profile. The jet diameter was depicted only over 20 pixels.

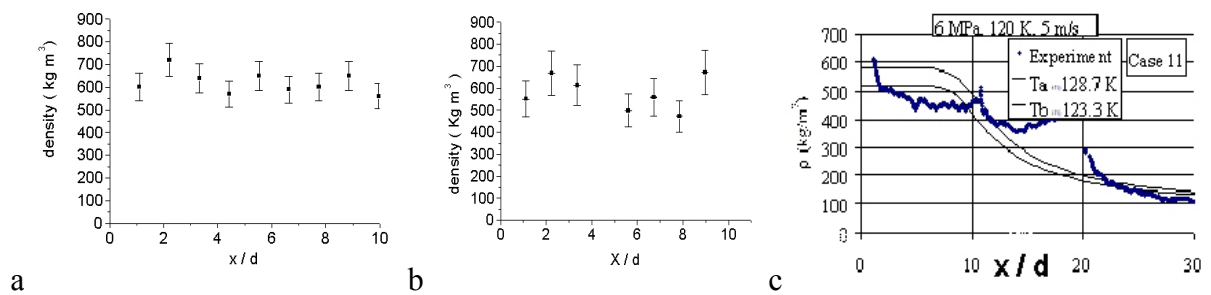


Figure 7 : longitudinal density evolution of a 100 K 6.0 MPa jet. -a- x-ray calculation of the average density (the jet is considered as an homogeneous density cylinder , -b- x-ray calculation of the on axis density of the jet, -c- CFD calculation and Raman measurement (dots) of the on axis density of the jet [14]

5. conclusion

The feasibility of x-ray diagnostic of nitrogen cryogenic jet in high pressure ambience has been demonstrated. The ACS detector – ICCD camera combination allowed to obtain

radiographs with sufficient contrast in all tested conditions (1.0 MPa 100 K, 4.0 MPa at 100,120 and 130 K, 6.0 MPa at 100,120 and 130 K). The x-ray spectrum evaluation and the development of a density calculation algorithm have been performed to obtain a first approximation of the jet density evolution in the near nozzle region. A rather good agreement between x-ray measurement and CFD data was achieved.

Work is in progress to optimize the x-ray diagnostic technique to obtain more precise density measurement in the near nozzle region of nitrogen jets or for other dense jets.

ACKNOWLEDGEMENT

This work is supported by the Région Centre and the Fédération EPEE.

REFERENCES

- [1] W.O.H.Mayer, A.Schik, C.Shweitzer, M.Schäffer, “ Injection and Mixing processes in high pressure LOX/GH2 rocket combustors”, 32th AIAA/ASME/SAE/ASEE joint propulsion conference, **2620**, (1996).
- [2] W.O.H.Mayer, H.J.Telaar, R.Branam, G.Schneider, J.Husson, “ characterization of Cryogenic injection at supercritical pressure”, 37 th AIAA Joint Propulsion Conference, AIAA 2001-3275, Salt Lake City, July 9-11, 2001.
- [3] Krehl and D.Warken, “Flash soft radiography – its adaptation to study of break-up mechanisms of liquid jets into a high density gas”, SPIE 19th ICHSPP Vol. **1358**, pp 162-173, (1990).
- [4] A.Birk, M. McQuaid, M. Gross, “Liquid core structure of evaporating sprays at high pressures – flash X-rays studies”, ICLASS, Rouen, France, **paper IV – 11, pp 459-466**, (1994).
- [5] L.Hure, E.Robert, C.Cachoncinlle, R.Viladrosa, J.M Pouvesle,” Spray and gaseous jet diagnostics using X-ray Induced Fluorescence Imaging and flash radiography”, SPIE 24th ICHSPP, pp **512-522** (2000).
- [6] A.G. MacPhee et al.,” X-ray imaging of shock Waves generated by high pressure fuel sprays “, Science, vol **295**,pp **1261-1263**, 15 Feb 2002
- [7] Y.Yue et al, ”Quantitative measurement of diesel fuel spray characteristics in the near –nozzle region using x-ray absorption “, Atomization and sprays vol **11**,pp 471-490,2001
- [8] C.F.Powell et al “ x-ray vision of fuel sprays”, ICLASS europe 2001.
- [9] R.D Woodward, K.N Garner, F.B Cheung, K.K Kuo,”Break-up phenomena of coaxial jet in the non-dilute region using real-time x-ray radiography “ AIAA **90-158**, AIAA 26 th Joint Propulsion conference, Orlando, July 16-18 1990
- [10] J.M.Pouvesle, C.Cachoncinlle, R.Viladrosa, E.Robert, A.Khacef, “ compact flash x-ray sources and their applications” NIMB, vol **113**, pp **134-140**, 1996
- [11] <http://physics.nist.gov/PhysRefData/contents.html>
- [12] B.Métay, E.Robert, R.Viladrosa, C.Cachoncinlle, J.M Pouvesle, W.Mayer, G.Schneider,” X-ray diagnostics of the near injector zone of cryogenic nitrogen jets at supercritical pressures”,to be published in SPIE 25 th ICHSSP 2002 NIST reference data :
- [13] R. Birsh, M.Marshall “ computation of Bremsstrahlung x-ray spectra and comparaison with spectra measured with a Ge(Li) detector”, Phys. Med. Biol. Vol. **24** n°3,pp **505-517**. 1979
- [14] W.O.H Mayer private communication.